Regenerated Fiber Bragg Gratings in Multicore Fiber for Multi-parameter Sensing

Javier Madrigal, David Barrera, and Salvador Sales, *Senior Member, IEEE*

***Abstract*—Multiple regenerated fiber Bragg gratings were inscribed in all the cores of a seven-core fiber in order to develop a multi-parameter sensor designed to operate at high temperatures. We experimentally showed the possibility of measuring strains of up to 1200 με, curvatures from 0º to 360º and temperatures up to 1000ºC, with a maximum curvature magnitude of at least 4.6 m^{-1} and a maximum sensibility of 96 pm/m^{-1}.**

***Index Terms*—Curvature, fiber Bragg gratings, multicore fiber, optical fiber sensors, strain, temperature.**

I. Introduction

Optical fiber sensors are now considered important due to their many advantages over their electrical counterparts, including: light weight, small size, high sensitivity, immunity to electromagnetic interference, chemical inertness, negligible ignition risk and the possibility of distributing sensors along the same fiber [1]. Fiber Bragg Gratings (FBGs) are a popular approach for optical fiber sensing and have been used in single core fibers for sensing applications and progressively applied in several fields such as civil engineering, the aerospace industry and medicine [2-6]. However, the common Type I FBG sensors are not suitable for high temperature environments as their refractive index modulation decays at temperatures over 400ºC, which rapidly reduces FBG reflectivity [7]. Regenerated fiber Bragg gratings (RFBGs) have been proposed to overcome this temperature limitation [8].

An RFBG consists of a seed FBG that undergoes an annealing process to make it able to withstand high temperatures. RFBGs are finding applications in an ever-growing number of fields, such as in turbines, combustors, nuclear reactors and aerospace projects [9]. To date, RBFGs have been used only for temperature monitoring, for example in structural fire tests [10] and foundry casting processes [11]. However, in structural health monitoring in civil engineering or aerospace applications it is often necessary to sense other parameters such as curvature or shape in order to avoid catastrophic failures. FBGs, and hence also RFBGs, in single core fibers are insensitive to curvature stimuli because the grating is placed in the center of the fiber. However, the spatial distribution of the cores in an MCF opens up new possibilities in optical sensing. The outer cores are sensitive to bending stimuli and can be used for curvature sensing, while the central core, which is insensitive to bending, can be used to measure temperature or strain. FBGs inscribed in multicore fibers (MCFs) have already been proposed for curvature and shape sensing [12-17]. In this paper, we propose to combine FBGs with MCFs and an annealing process [18] in order to create an RFBG-based multiparameter sensor capable of measuring strain, curvature and temperatures up to 1000ºC. The proposed sensor can be of great interest for monitoring structures that could be deformed and bent while they are exposed to high temperatures, e.g. structures during fire testing, aerospace vehicles parts and components of power plants or other industrial facilities such as pipes, vessels and turbines, among others [10, 19-23].

Several samples of the sensor were produced for experimental characterization. The FBG inscription technique used to implement the sensors and the annealing process used to create the RFBGs are described in Section 2. Section 3 reports on the high temperature and room-temperature strain characterization experimental results, while the curvature characterization is described in Section 4. The sensors' behavior under curvature at high temperatures is reported in Section 5, and our conclusions are summarized in Section 6.

II. Regenerated FBG-based Sensor in a Multicore Fiber.

The MCF had seven cores arranged in a hexagonal pattern with one core in the center. Fiber cladding diameter was 125μm and core spacing 35 μm. Prior to FBG inscription, the fiber was hydrogen loaded at 50 bar at room temperature for at least two weeks to increase its photosensitivity. The phase mask technique [24] was used to inscribe the same FBG in all the cores of a commercial multicore optical fiber (Fibercore SM-7C1500) carried out by a 244 nm CW argon-ion laser. A set of

This work was partially supported by the Spanish Ministry of Economy and Competitiveness under the DIMENSION TEC2017 88029- R Project and partially by the *Generalitat Valenciana* by the PROMETEO 2017/103 Research Excel lency Award and IDI/FEDER/2018 GVA *Infraestructura*. J. Madrigal was supported by a Universitat Politècnica de València scholarship PAID-01-18 and D. Barrera by a Spanish MICINN Fellowship IJCI- 2017-32476. *(Corresponding author: Javier Madrigal.)* J. Madrigal and S. Sales are with the Photonics Research Labs, ITEAM Research Institute, *Universitat Politècnica de València*, Valencia 46022, Spain (e-mail: jamadmad@iteam.upv.es; ssales@dcom.upv.es). D. Barrera is with the Department of Electronics, University of Alcalá, Alcalá de Henares 28805, Spain (e-mail: david.barrera@uah.es).

lenses was used to adjust the laser beam diameter to inscribe all cores simultaneously. A tracking system kept the beam in the center of the fiber during the inscription process [25]. Figure 1 shows the inscription setup and the core arrangement inside the fiber. The cores were numbered and the same number reference was used for all the measurements. For individual core measurement, the MCF was coupled to a seven single core fibers by a commercial fan-in/out device [26].

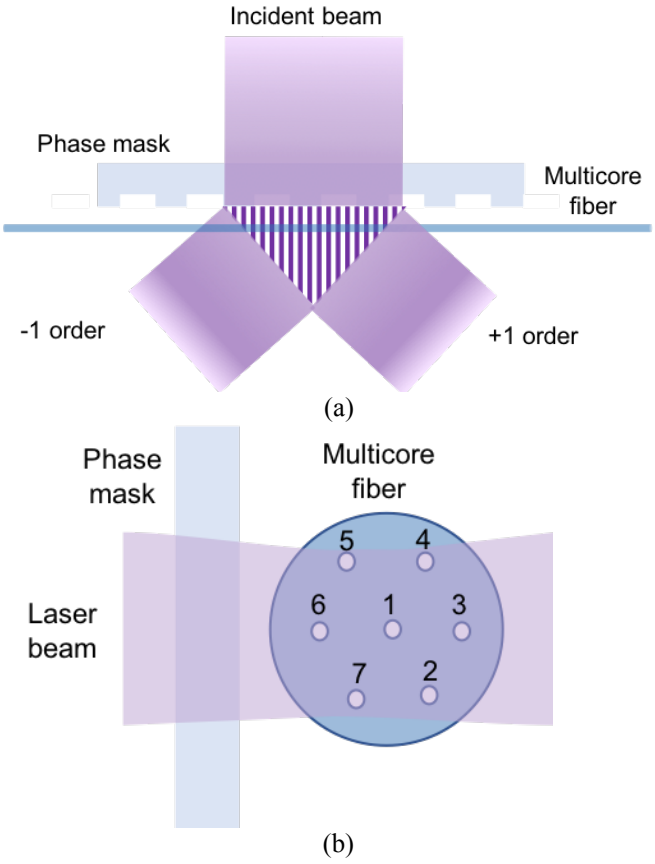

Fig.1 Inscription of FBGS using a phase mask . (a) Grating scheme. (b) Cross section of fiber during inscription and core arrangement inside the fiber.

To obtain the RFBGs, the inscribed FBGs were subjected to sequential thermal processing in a small tubular furnace. Only the part of the fiber that contains the FBGs was placed in the furnace to facilitate future handling operations. In the first step the FBGs were heated from ambient temperature to 1000ºC at 6ºC/min, after which temperature was kept constant for at least 2.5 hours. The RFBGs were allowed to cool to room temperature. The FBGs in cores #1, #2, #3 and #6 were continually monitored during the process by means of the four channels of a Micron Optics sm130 Optical Sensing Interrogator. Fig. 2 shows the furnace temperature sequence and the power reflected by each FBG during the process. Initially, the reflected power remained constant. At close to 700ºC the FBGs started to decay rapidly as temperature increased. The FBGs disappeared completely as the RFBGs appeared. Fig. 3 shows the RFBG spectra at room temperature at the end of the regeneration process.

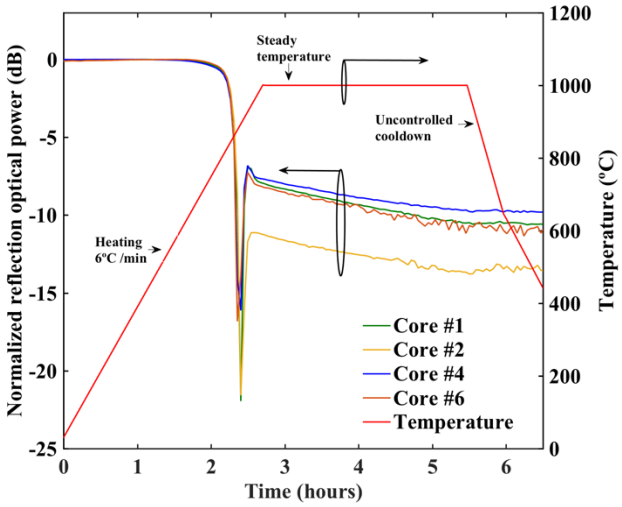

Fig. 2 Reflection optical power for the FBG in cores #1, #2, #4 and #6 for each temperature during the regeneration process.

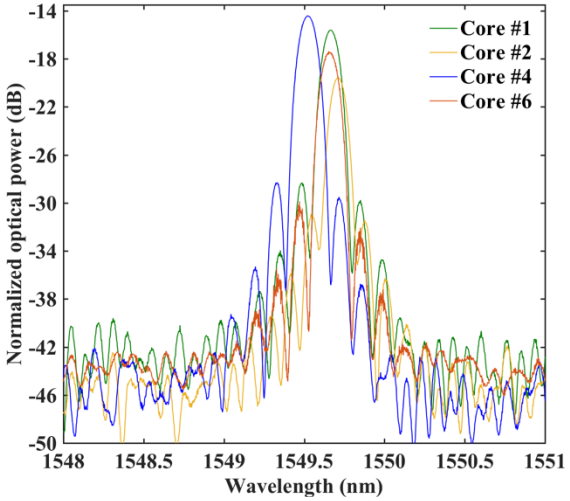

Fig. 3 RFBG spectra in four cores. Those in the other cores had similar spectra.

III. TEMPERATURE AND STRAIN CHARACTERIZATION

Due to the fiber geometry and the core arrangement, core #1was not affected by curvature changes and could be used as a temperature sensor. The RFBGs were placed in a straight horizontal position inside the tube furnace and gradually heated from 24ºC to 1000ºC to characterize the RFBGs for high temperatures sensing. Fig. 4 shows the wavelength shift of the RFBG in core #1 with reference to 24ºC. A cubic polynomial fitting was applied using the equation:

$$\Delta\lambda(T) = -3.46\cdot10^{-9}\cdot T^3 + 8.29\cdot10^{-6}\cdot T^2 + 0.099T - 0.24 \quad (1)$$

where $\Delta\lambda$ is the wavelength shift in nanometers and T is the temperature expressed in Celsius degrees. The coefficient of determination obtained is R^2=0.99, which indicates that the wavelength shift shows good quadratic agreement with temperature.

The section of fiber with the RFBGs was fixed between two translation stages with cyanoacrylate adhesive for strain characterization. One of the stages was moved by a micrometer screw to induce a strain in the fiber. Since the regeneration process weakens the fiber, we previously determined its breaking strength, which was found to be 1300 με. The strain was thus limited to 1200 με to ensure the fiber survived the experiments. When the fiber was straight, all the cores underwent the same strain. Fig. 5 shows core #1 RFBG wavelength shift with reference to the fiber without strain. A linear fit was applied using the equation:

$$\Delta\lambda(\varepsilon) = k \cdot \varepsilon \tag{2}$$

Where Δλ is the wavelength shift, in nanometers, k is the sensitivity and ε is the strain in microstrain. The strain sensitivity obtained by linear fitting was k=0.00102 nm/με. The coefficient of determination obtained, R^2=0.99 indicates a good linear dependence.

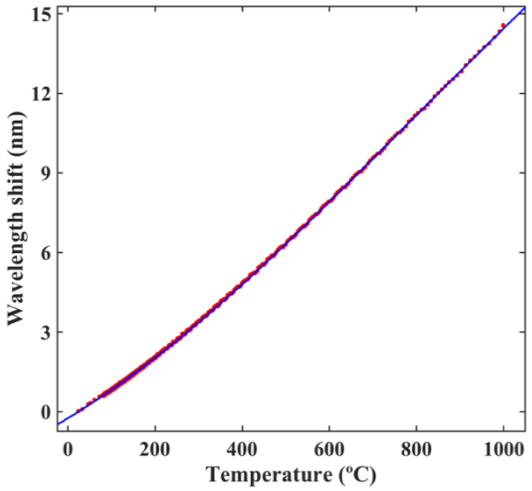

Fig.4. Wavelength shift of RFBG in core #1 versus temperature from 24ºC to 1000ºC. The solid line is the fitted curve.

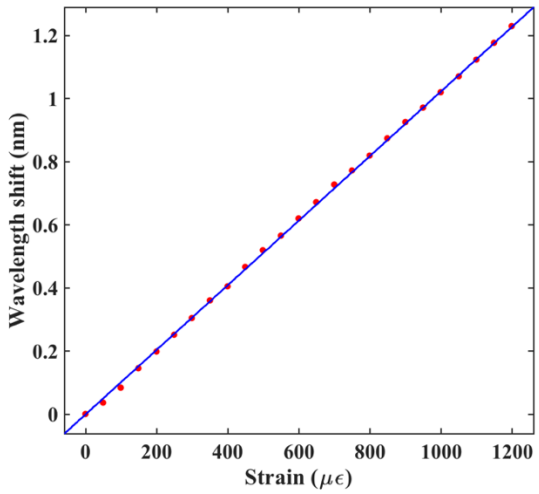

Fig.5 Wavelength shift of RFBG in core #1 versus the strain applied. The solid line is the fitted line.

IV. CURVATURE CHARACTERIZATION

The setup shown in Fig 6 was used to measure curvature. The fiber was placed on a metal strip of given thickness with the RFBGs in the center. Using the rotators on both sides simultaneously, the cores' spatial orientation could be modified from 0º to 360º. Curvature was induced in the metal strip by moving one translation stage and was calculated using the following equation [15,16]:

$$\sin\left(\frac{L \cdot C}{2}\right) = \frac{(L - D) \cdot C}{2} \tag{3}$$

where L is the length of the metal strip, D is the forward distance of the moving stage and C is the curvature. For this setup, L=15 cm, D varied from 0 to 3mm and the metal strip was 0.3mm thick.

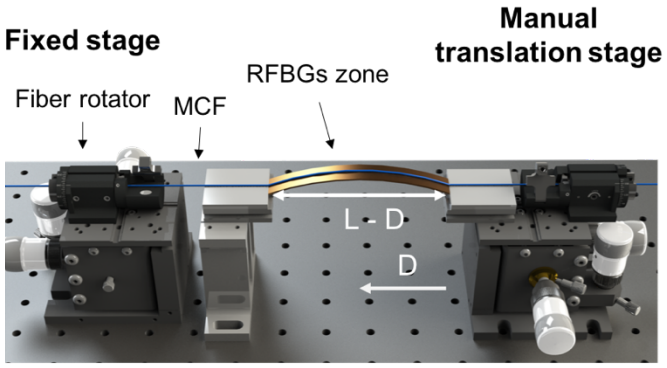

Fig 6. Setup for curvature experiments. Left stage remains fixed and right stage is moved by rotating a micrometer screw.

Prior to measuring curvature, we placed cores #5 and #2 on top and bottom position respectively using the fiber rotators. The curvature of the metal strip was increased from 2.3 m^{-1} to 4.6 m^{-1} and the wavelength shift was measured in all the cores. Fig. 7 shows the wavelength shift of the cores in relation to the curvature. The wavelength shift is referenced to Bragg wavelength when D=0.5mm. Core #1 shows a negligible wavelength shift because it is in the neutral line and does not suffer any strain. The RFBG in core #1 can thus be used to compensate the wavelength shift induced by the temperature changes. In the remaining cores, the wavelength shift shows a linear behavior with curvature magnitude for a fixed curvature direction. A linear fit was applied to curvature magnitude measurements:

$$\Delta\lambda(C) = a \cdot C + b \tag{4}$$

where Δλ is the wavelength shift, in nanometers, and C is the curvature magnitude , expressed in m^{-1}, and a and b are the fitting coefficients. Table 1 shows the fitting coefficients and the determination coefficient R^2 for each core. The position of the cores with reference to the neutral line affects the RFBGs' wavelength shift. The cores below the neutral lines experience compressive strains while those above experience tensile strains that induce negative and positive wavelength shifts respectively. Also, the strain induced by the curvature, and thus the measured wavelength shift, depends on the distance of the core from the neutral line. This behavior can be used for

curvature magnitude and direction sensing and for shape sensing [15].

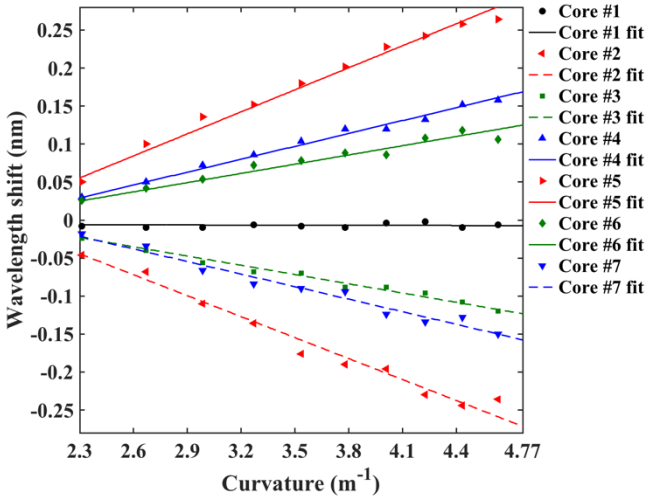

Fig.7. Wavelength shift vs curvature in all the cores. The solid and dashed lines are the fitted curves.

TABLE I
CURVATURE MAGNITUDE LINEAR FITTING EQUATION COEEFICIENTS

Core	*a*	*b*	R^2
1	-0.00043	-0.0052	<0.20
2	-0.092	0.17	0.98
3	-0.040	0.07	0.98
4	0.056	-0.10	0.99
5	0.096	-0.16	0.98
6	0.040	-0.07	0.96
7	-0.055	0.10	0.98

The differences in curvature sensitivities between cores 4 and 6, and 3 and 7 is produced by a slight misalignment of the cores relative to the vertical position of approximately 4.3º.

In order to characterize the sensor response in different curvature directions, we then fixed the curvature and rotated the fiber from θ=0º to θ=360º in steps of 15º and measured the wavelength shift of each RFBG. Fig. 8 shows the wavelength shift of the RFBGs in relation to the mean of the maximum and the minimum wavelength shift in the complete rotation range. It can be seen that the wavelength shifts due to curvature direction changes have a sinusoidal behavior. A sinusoidal curve fitting was applied:

$$\Delta\lambda(\theta) = a \cdot \sin(b \cdot \theta + c) \quad (5)$$

where $\Delta\lambda$ is the wavelength shift, in nanometers, θ is the angle of rotation expressed in degrees and a, b and c are the fitting coefficients. These coefficients are summarized in Table 2. The coefficients showed in Table 1 and Table 2 indicate a non-curvature dependent wavelength shift in core #1. The slight wavelength shifts in core #1 are due to temperature changes and systematic errors. In the curvature magnitude measurements, the core #1 wavelength shift mean value was -0.0067 nm and the standard deviation was 0.0035 nm. Also, in the curvature direction measurements, the core #1 wavelength shift mean value was 0.0012 nm and the standard deviation value was 0.0028 nm.

TABLE II
CURVATURE DIRECTION FITTING EQUATION COEFFICIENTS

Core	*a*	*b*	*c*	R^2
1	0.002	0.008	-0.487	<0.20
2	0.240	0.016	-1.338	0.99
3	0.228	0.016	-2.443	0.99
4	0.233	0.016	2.729	0.99
5	0.244	0.016	1.813	0.99
6	0.228	0.016	0.642	0.99
7	0.233	0.016	-0.426	0.99

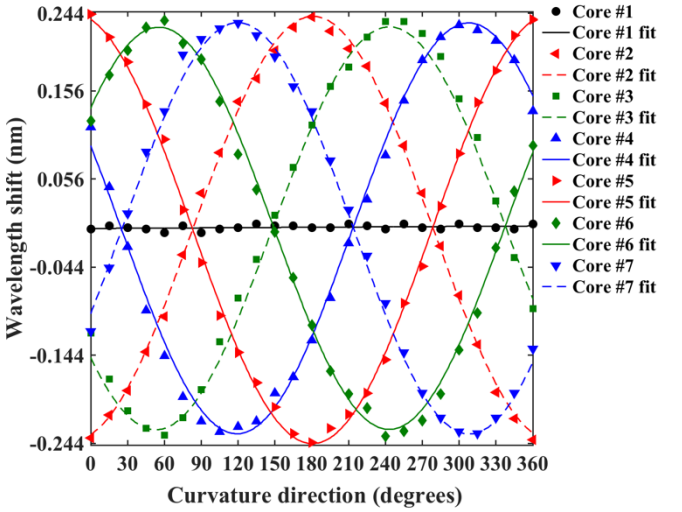

Fig.8. Wavelength shift vs RFBG curvature direction. The solid lines are the fitted curves.

In order to simultaneously determine curvature magnitude and direction, the curvature direction is first determined by observing the relation between the wavelength shifts in each core that is unique for any curvature direction. The curvature magnitude is then proportional to the wavelength shift [16].

V. HIGH TEMPERATURE CURVATURE CHARACTERIZATION

To study the behavior of the sensor at high temperatures, we measured curvature magnitude at temperatures of 100ºC, 300ºC and 500º C. To heat the fiber without damaging the characterization setup a hot air gun was used. We measured the wavelength shift of the RFBGs in cores #4 and #7. In order to compensate for the shift due to a temperature increase, the peak RFBG wavelength in core #1 was used as reference. Fig. 9 compares the wavelength shift measured for curvatures from 1.9 m-1 to 4.6 m-1 at different temperatures.

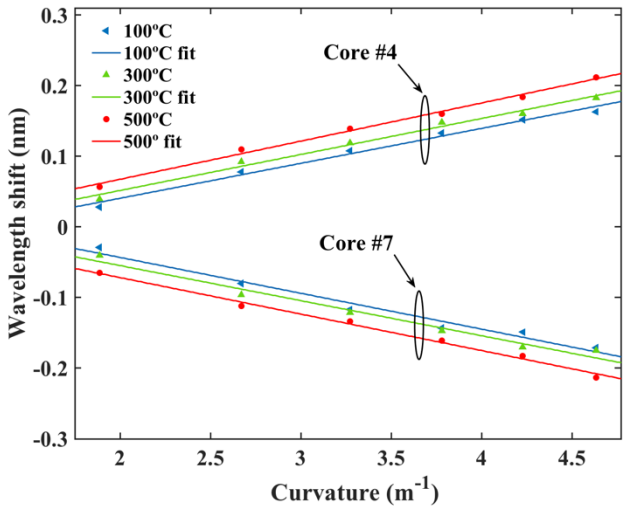

Fig.9. Wavelength shift of the RFBGs in cores #4 and #7 vs curvature magnitude at different temperatures.

As Fig 9 shows, in this case the slopes of the wavelength shift in the cores are similar at all three temperatures, so that no significant variations in the sensitivity to curvature are seen when the temperature increases. This is because the strain sensitivity changes caused by temperature are not large enough to significantly modify the curvature sensitivity when the fiber is heated to 500ºC [27, 28]. Fig. 9 shows a slight bias shift within the temperature. The curvature at high temperatures was measured using a hot air gun in order to heat the fiber. The airflow moved the fiber and produced the small wavelength drifts.

VI. Conclusion

To our knowledge, this is the first time RBFGs have been used in multicore fibers to measure temperature, strain and curvature at high temperatures to obtain a multiparameter sensor able to operate in extreme environmental conditions. A sensor for inscribing fiber Bragg Gratings was developed in a seven core fiber and we then successfully regenerated the gratings by an annealing process. The sensor was first characterized for temperatures up to 1000ºC, obtaining a cubic response. We then characterized the sensor at room temperature for strains up to 1200 με and curvature magnitudes up to 4.6m^{-1} in directions from 0º to 360º. The strain sensitivity was found to be 1.02 pm/με and curvature sensitivity was 96 pm/m^{-1}. The central core of the fiber was not sensitive to curvature and could be used for temperature and curvature measurements. We also showed that the sensor can measure curvature at high temperatures and studied the influence of temperature on the sensitivity of these parameters. The results obtained show that no significant changes in curvature magnitude sensitivity when temperature increases.

References

[1] B. Lee, "Review of the present status of optical fiber sensors," *Optical Fiber Technology*, vol. 9, no. 2, pp. 57–79, 2003.

[2] A. Kersey, M. Davis, H. Patrick, M. Leblanc, K. Koo, C. Askins, M. Putnam, and E. Friebele, "Fiber grating sensors," *Journal of Lightwave Technology*, vol. 15, no. 8, pp. 1442–1463, 1997.

[3] H.-N. Li, D.-S. Li, and G.-B. Song, "Recent applications of fiber optic sensors to health monitoring in civil engineering," *Engineering Structures*, vol. 26, no. 11, pp. 1647–1657, 2004.

[4] B. Torres, I. Payá-Zaforteza, P. A. Calderón, and J. M. Adam, "Analysis of the strain transfer in a new FBG sensor for Structural Health Monitoring," *Engineering Structures*, vol. 33, no. 2, pp. 539–548, 2011.

[5] V. Mishra, N. Singh, U. Tiwari, and P. Kapur, "Fiber grating sensors in medicine: Current and emerging applications," *Sensors and Actuators A: Physical*, vol. 167, no. 2, pp. 279–290, 2011.

[6] I. Mckenzie and N. Karafolas, "Fiber optic sensing in space structures: the experience of the European Space Agency (Invited Paper)," *17th International Conference on Optical Fibre Sensors*, 2005.

[7] T. Erdogan, V. Mizrahi, P. J. Lemaire, and D. Monroe, "Decay of ultraviolet-induced fiber Bragg gratings," *Journal of Applied Physics*, vol. 76, no. 1, pp. 73–80, 1994.

[8] J. Canning, S. Bandyopadhyay, P. Biswas, M. Aslund, M. Stevenson, and K. Cook, "Regenerated Fibre Bragg Gratings," *Frontiers in Guided Wave Optics and Optoelectronics*, pp. 363–384, Jan. 2010.

[9] D. Barrera, V. Finazzi, J. Villatoro, S. Sales, and V. Pruneri, "Packaged Optical Sensors Based on Regenerated Fiber Bragg Gratings for High Temperature Applications," *IEEE Sensors Journal*, vol. 12, no. 1, pp. 107–112, 2012.

[10] B. T. Górriz, I. Payá-Zaforteza, P. C. García, and S. S. Maicas, "New fiber optic sensor for monitoring temperatures in concrete structures during fires," *Sensors and Actuators A: Physical*, vol. 254, pp. 116–125, 2017.

[11] M. Lindner, E. Tunc, K. Weraneck, F. Heilmeier, W. Volk, M. Jakobi, A. W. Koch, and J. Roths, "Regenerated Bragg Grating Sensor Array for Temperature Measurements During an Aluminum Casting Process," *IEEE Sensors Journal*, vol. 18, no. 13, pp. 5352–5360, Jan. 2018.

[12] D. Barrera, J. Hervás, I. Gasulla, and S. Sales, "Enhanced accuracy sensors using multicore optical fibres based on RFBGs for temperatures up to 1000°C," *Sixth European Workshop on Optical Fibre Sensors*, 2016.

[13] A. Fender, W. N. Macpherson, R. R. J. Maier, J. S. Barton, D. S. George, R. I. Howden, G. W. Smith, B. J. S. Jones, S. Mcculloch, X. Chen, R. Suo, L. Zhang, and I. Bennion, "Two-Axis Temperature-Insensitive Accelerometer Based on Multicore Fiber Bragg Gratings," *IEEE Sensors Journal*, vol. 8, no. 7, pp. 1292–1298, 2008.

[14] D. Barrera, I. Gasulla, and S. Sales, "Multipoint Two-Dimensional Curvature Optical Fiber Sensor Based on a Nontwisted Homogeneous Four-Core Fiber," *Journal of Lightwave Technology*, vol. 33, no. 12, pp. 2445–2450, 2015.

[15] D. Barrera, J. Madrigal, and S. Sales, "Long Period Gratings in Multicore Optical Fibers for Directional Curvature Sensor Implementation," *Journal of Lightwave Technology*, vol. 36, no. 4, pp. 1063–1068, 2018.

[16] J. P. Moore and M. D. Rogge, "Shape sensing using multi-core fiber optic cable and parametric curve solutions," *Optics Express*, vol. 20, no. 3, p. 2967, 2012.

[17] H. Zhang, Z. Wu, P. P. Shum, R. Wang, X. Q. Dinh, S. Fu, W. Tong, and M. Tang, "Fiber Bragg gratings in heterogeneous multicore fiber for directional bending sensing," Journal of Optics, vol. 18, no. 8, p. 085705, 2016.

[18] J.Madrigal, D.Barrera, P.A Calderón, S. Sales. "Regenerated multicore fibre Bragg gratings for structural health monitoring in harsh environments", *18th European Conference on Spacecraft Structures Materials and Environmental Testing, 2018.* (Not published)

[19] K. Cook, J. Canning, S. Bandyopadhyay, M. Lancry, C. Martelli, T. Jin, and A. Csipkes, "Overview of high temperature fibre Bragg gratings," 2017 Conference on Lasers and Electro-Optics Pacific Rim (CLEO-PR), 2017.

[20] R. J. Black, J. M. Costa, L. Zarnescu, D. A. Hackney, B. Moslehi, and K. J. Peters, "Fiber-optic temperature profiling for thermal protection system heat shields," Optical Engineering, vol. 55, no. 11, p. 114101, 2016.

[21] H.-E. Joe, H. Yun, S.-H. Jo, M. B. Jun, and B.-K. Min, "A review on optical fiber sensors for environmental monitoring," International Journal of Precision Engineering and Manufacturing-Green Technology, vol. 5, no. 1, pp. 173–191, 2018.
[22] G. Sposito, C. Ward, P. Cawley, P. Nagy, and C. Scruby, "A review of non-destructive techniques for the detection of creep damage in power plant steels," NDT & E International, vol. 43, no. 7, pp. 555–567, 2010.
[23] W. Ecke and M. W. Schmitt, "Fiber Bragg Gratings in Industrial Sensing," in Optical Fiber Communication Conference/National Fiber Optic Engineers Conference 2013, OSA Technical Digest (online) (Optical Society of America, 2013), paper OM3G.1.
[24] K. Hill and G. Meltz, "Fiber Bragg grating technology fundamentals and overview," *Journal of Lightwave Technology*, vol. 15, no. 8, pp. 1263–1276, 1997.
[25] I. Gasulla, D. Barrera, J. Hervás, and S. Sales, "Spatial Division Multiplexed Microwave Signal processing by selective grating inscription in homogeneous multicore fibers," *Scientific Reports*, vol. 7, no. 1, 2017.
[26] http://www.optoscribe.com
[27] M. J. Odwyer, C.-C. Ye, S. W. James, and R. P. Tatam, "Thermal dependence of the strain response of optical fibre Bragg gratings," *Measurement Science and Technology*, vol. 15, no. 8, pp. 1607–1613, 2004.
[28] G.-Y. Li and B.-O. Guan, "The strain response of chemical composition gratings at high temperatures," *Measurement Science and Technology*, vol. 20, no. 2, p. 025204, 2008.

Javier Madrigal received the M.Sc. degree in telecommunications engineering from Universitat Politècnica de València, Valencia, Spain, in 2015. He is currently working toward the Ph.D. degree in communications engineering. Since 2015, he has been working as a Researcher with Photonics Research Labs, ITEAM Research Institute, where he has been involved in the design and fabrication of fiber Bragg gratings. His research interests include multicore fibers, optical fiber sensors, long period gratings, and tilted fiber Bragg gratings.

David Barrera received the M.Sc. and Ph.D. degrees from the Universitat Politècnica de València, Valencia, Spain, in 2008 and 2013, respectively. He is currently a Postdoctoral Researcher with the Universidad de Alcalá, Alcalá de Henares, Spain. His current research interests include optical fiber sensors, fiber Bragg gratings, and multicore optical fibers.

Salvador Sales (S'93–M'98–SM'04) received the M.Sc. and Ph.D. degrees from the Universitat Politècnica de València, Valencia, Spain. Since 2007, he has been a Professor with the ITEAM Research Institute, Universitat Politècnica de València. He is a coauthor of more than 125 journal papers and 300 international conference papers. He has been collaborating and leading some national and European research projects since 1997. His main research interests include optoelectronic signal processing for optronic and microwave systems, optical delay lines, fiber Bragg gratings, WDM and SCM lightwave systems, and semiconductor optical amplifiers. He was the recipient of the Annual Award of the Spanish Telecommunication Engineering Association for the best Ph.D. on optical communication.